

## Mono- versus Binuclear Copper(II) Complexes in Phosphodiester Hydrolysis

Katalin Selmeczi,<sup>[a,c]</sup> Michel Giorgi,<sup>[c]</sup> Gábor Speier,<sup>[a,b]</sup> Etelka Farkas,<sup>[d]</sup> and Marius Réglér\*<sup>[c]</sup>**Keywords:** Catalysis / Dinuclear copper(II) complex / Enzyme mimics / Phosphate ester hydrolysis / Tripodal ligands

Mono- and dinuclear copper(II) complexes [Cu(L<sup>1</sup>OH)]-(CF<sub>3</sub>SO<sub>3</sub>)<sub>2</sub> (**1**) and [Cu<sub>2</sub>(L<sup>2</sup>O)](CF<sub>3</sub>SO<sub>3</sub>)<sub>3</sub> (**2**) have been synthesized and characterized by X-ray crystallography. Complexes **1** and **2** were then tested as catalysts for the hydrolysis of bis(*p*-nitrophenyl)phosphate (BNPP). At pH 6, the dinuclear complex **2** was found to be 20-fold more active than complex **1** and the reaction up to 600-fold faster than the un-promoted reaction. On the basis of potentiometric studies, we were

able to demonstrate that the bis(aqua)copper complex was the active species by the formation of a ternary complex in which one copper atom binds to a hydroxide and the second, to the substrate. We also propose that BNPP reacts with the bis(aqua)copper complex to give a stable, hydrolytically inactive BNPP-2 complex (**3**).

(© Wiley-VCH Verlag GmbH & Co. KGaA, 69451 Weinheim, Germany, 2006)

## Introduction

During the last decade, there has been increasing interest in the development of metal complexes which promote the hydrolysis of phosphate ester linkages.<sup>[1-2]</sup> The main approach developed in this domain concerns the design of functional models for hydrolytic metalloenzymes. Beside their important roles in the understanding of their mechanisms, the development of hydrolytic metalloenzyme mimics are of great importance in biotechnology for the design of synthetic nucleases which could be used as artificial restriction enzymes. On the other hand, since a number of phosphate esters and related phosphorus(V) compounds are used in agriculture as pesticides or, unfortunately, as potent nerve agents in chemical weaponry (mustard gases), the development of catalytic systems able to hydrolyze and destroy such compounds is of considerable environmental and medicinal importance.

Among the metalloenzymes which catalyze the hydrolysis of the phosphate ester linkage, metallonucleases are important because they are ubiquitous and essential for living organisms.<sup>[3]</sup> Certainly, due to its high natural abundance and

good Lewis acid properties, Mg<sup>2+</sup> is the most important metal encountered in nuclease active sites. Multinuclear transition metal centers with Zn<sup>2+</sup>, Mn<sup>2+</sup> and Fe<sup>2+</sup> are often present too. As examples, in enzymes which hydrolyze phosphodiester into phosphomonoesters, the active site of alkaline phosphatase contains a dinuclear Zn<sup>2+</sup> core,<sup>[4]</sup> while the active site present in purple acid phosphatases (PAPs) contains one Fe<sup>3+</sup> associated to a Fe<sup>2+</sup> (or Zn<sup>2+</sup>, Mn<sup>2+</sup>).<sup>[5]</sup> In the commonly disclosed mechanism, one of the metal ions (the one with the highest Lewis acidity) favors the formation and co-ordination of a hydroxide ion at physiological pH, while the second one activates the phosphate ester group for intramolecular nucleophilic attack by the adjacent hydroxide. On the basis of this mechanism, nuclease mimics incorporating dinuclear metal centers with Co,<sup>[6,7]</sup> Ln,<sup>[8,9]</sup> Zn<sup>[10,11]</sup> and Fe<sup>[12]</sup> were recently published as efficient bioinspired catalysts for phosphoester hydrolysis.

While the copper ion has never been identified as a cofactor in natural nucleases, Cu<sup>2+</sup> exhibits some interesting features rendering it attractive for artificial nucleases: (i) Cu<sup>2+</sup> is substitutionally labile and at the same time a strong Lewis acid necessary for the activation of the phosphodiester bond towards nucleophilic attack and (ii) Cu<sup>2+</sup> lowers the pK<sub>a</sub> of coordinated water, thereby providing metal-bound hydroxide at near-neutral pH. That is why binuclear<sup>[13,14]</sup> complexes of Cu<sup>2+</sup> have also been described as efficient bioinspired catalysts in phosphoester hydrolysis.

The importance of nuclearity (mononuclear vs. dinuclear) was clearly demonstrated for Fe<sup>3+</sup>.<sup>[12]</sup> The situation is less clear for copper since mononuclear Cu<sup>2+</sup> complexes were also reported in the literature as agents with good activity.<sup>[15,16]</sup> We report in this paper the kinetics of BNPP hydrolysis by the dinuclear [Cu<sub>2</sub>(L<sup>2</sup>O)](CF<sub>3</sub>SO<sub>3</sub>)<sub>3</sub> (**2**), in order to study the influence of the nuclearity of copper com-

[a] Research Group for Petrochemistry, Hungarian Academy of Sciences, 8200 Veszprém, Hungary

[b] Department of Organic Chemistry, University of Veszprém, 8201 Veszprém, Hungary

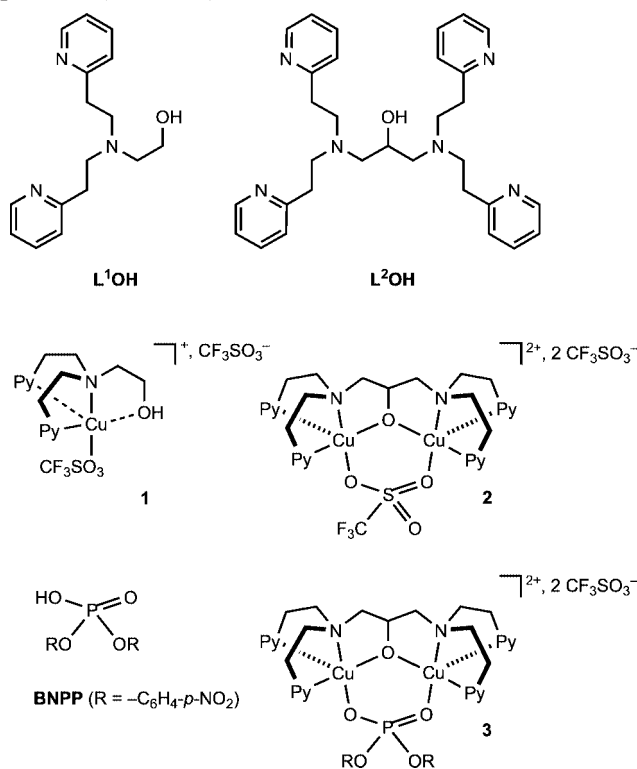
[c] Chimie, Biologie et Radicaux Libres, UMR CNRS 6517, Faculté des Sciences et Techniques, case 432, Université Paul Cézanne Aix-Marseille III, Avenue Escadrille Normandie-Niemen, 13397 Marseille Cedex 20, France  
Fax: +33-491-983-208  
E-mail: marius.reglier@univ.u-3mrs.fr

[d] Department of Inorganic and Analytical Chemistry, Faculty of Science, University of Debrecen, 4010 Debrecen, Hungary

plexes, including a quantitative comparison with the mononuclear parent complex  $[\text{Cu}(\text{L}^1\text{OH})](\text{CF}_3\text{SO}_3)_2$  (**1**).

## Results and Discussion

**Synthesis:** Michael addition of 2-ethanolamine or 1,3-diamino-2-hydroxypropane to freshly distilled 2-vinylpyridine in methanol/acetic acid leads to ligands  $\text{L}^1\text{OH}$  and  $\text{L}^2\text{OH}$ , respectively.<sup>[17]</sup> The corresponding copper(II) complexes **1** and **2** were obtained in good yields by treatment with 1 equiv. of ligands  $\text{L}^1\text{OH}$  and  $\text{L}^2\text{OH}$  in dichloromethane with 1 and 2 equiv. of copper(II) triflate, respectively.<sup>[18]</sup> Complex **3** was prepared by mixing 1 equiv. of complex **2** in water with 1 equiv. of BNPP in methanol at room temperature (Scheme 1).



Scheme 1.

**Crystal Structures:** Crystal data for complexes **1** and **3**, together with details of the X-ray diffraction experiment, are reported in Table 5.

Single crystals of  $[\text{Cu}(\text{L}^1\text{OH})](\text{CF}_3\text{SO}_3)_2$  (**1**) suitable for X-ray diffraction analysis were obtained by slow diethyl ether vapor diffusion into a saturated acetone solution of the copper complex **1**.  $[\text{Cu}(\text{L}^1\text{OH})](\text{CF}_3\text{SO}_3)_2$  (**1**) is a mononuclear complex with a five-coordinate copper(II) cation (Figure 1). The geometry around the copper(II) ion is clearly a quite perfect square pyramid as it can be seen from the geometric parameters and the  $\tau$  factor which is equal to 0.04.<sup>[19]</sup> The equatorial positions are occupied by one pyridine N atom (N3) and the nitrogen N1 and oxygen O19 of the ethanolamine moiety. The fourth equatorial ligand is

the oxygen atom of a triflate counterion. The nitrogen N2 of the second pyridine occupies the axial coordination site at a distance equal to 2.171(4) Å from the copper, which is typically somewhat longer than the equatorial copper to pyridine distance [ $d_{\text{Cu-N3}} = 1.979(4)$  Å]. The deviation of the copper atom from the mean basal plane defined by atoms N1, N3, O1 and O19 is equal to 0.291 Å.

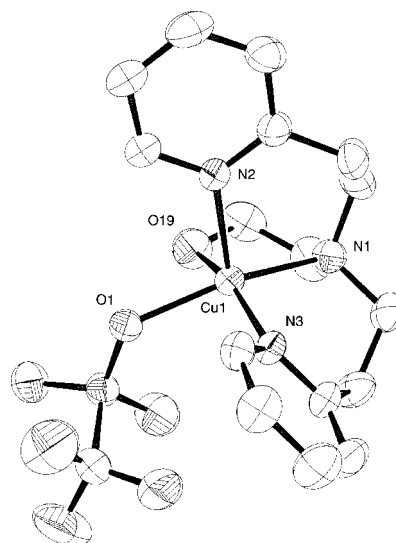


Figure 1. ORTEP perspective view of copper(II) complex  $[\text{Cu}(\text{L}^1\text{OH})](\text{CF}_3\text{SO}_3)_2$  (**1**). The H atoms and one  $\text{CF}_3\text{SO}_3^-$  counterion are omitted for clarity. Bond lengths are in Å: Cu–N1 2.044(4), Cu–N2 2.171(4), Cu–N3 1.979(4), Cu–O1 2.042(3), Cu–O19 1.973(4). Bond angles are in °: N1–Cu–N2 96.93(16), N3–Cu–O1 88.51(15), N3–Cu–N2 100.28(19), N3–Cu–N1 95.26(17), O1–Cu–N2 98.14(15), O19–Cu–N1 84.54(18), O19–Cu–N2 98.4(2), O1–Cu–N1 163.55(16), O19–Cu–O1 86.77(17), O19–Cu–N3 161.21(18). Numbers in parentheses are the estimated standard deviation in the least significant digits.

For the complex **2**, suitable crystals for X-ray diffraction analysis were obtained by slow diethyl ether vapor diffusion into a saturated dichloromethane solution. The structure of  $[\text{Cu}_2(\text{L}^2\text{O})](\text{CF}_3\text{SO}_3)_3$  (**2**), already described in a previous paper,<sup>[18]</sup> consists of a binuclear complex with two tetragonally coordinated  $\text{Cu}^{\text{II}}$  ions bridged in the equatorial positions by the alkoxide and triflate ligands (Figure 2). The Cu–Cu distance was found to be 3.699(3) Å. This is somewhat longer than that found e.g. in the similar  $[\text{Cu}_2(\text{L}^2\text{O})(\text{OMe})](\text{PF}_6)_2$  [2.995(2) Å].<sup>[20]</sup> The two positions in the basal plane of the copper ions are occupied by one of the pyridine nitrogen atoms and the aliphatic nitrogen of the ligand  $\text{L}^2\text{OH}$ . The other two equatorial positions are occupied by the oxygen atoms O1 of the ligand  $\text{L}^2\text{OH}$  and O2 of the triflate anion. As in complex **1**, the geometry around both coppers is a square pyramidal ( $\tau = 0.11$ ) and the distance of the Cu–atoms to the mean plane defined by atoms O1, O2, N1 and N2 is equal to 0.308 Å. The axial pyridine N3 donor, which is bound to the  $\text{Cu}^{\text{II}}$  atom at a distance of 2.179(4) Å, is a bit longer than the equatorial pyridine donor N2 [ $\text{Cu1-N2}$  2.009(3) Å]. The bond lengths

and bond angles of **2** shows similarities to other dicopper complexes with ligands derived from 1,3-diamino-2-hydroxypropane.<sup>[20–22]</sup>

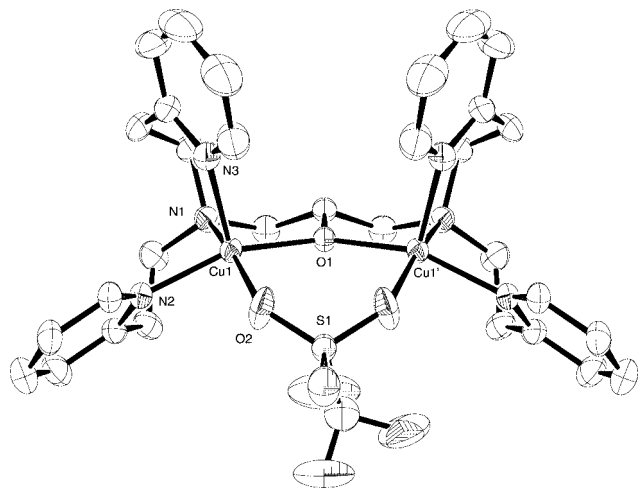


Figure 2. ORTEP perspective view of the copper(II) complex  $[\text{Cu}(\text{L}^2\text{O})](\text{CF}_3\text{SO}_3)_2$  (**2**). The H atoms and 2  $\text{CF}_3\text{SO}_3^-$  counterion are omitted for clarity. Bond lengths are in Å: Cu1–O1 1.9695(12), Cu1–N2 2.009(3), Cu1–N1 2.032(3), Cu1–O2 2.047(3), Cu1–N3 2.179(4). Bond angles are in °: O1–Cu1–N2 159.45(14), O1–Cu1–N1 87.04(12), N2–Cu1–N1 94.17(12), O1–Cu1–O2 90.54(12), N2–Cu1–O2 83.10(13), N1–Cu1–O2 165.31(15), O1–Cu1–N3 104.69(11), N2–Cu1–N3 95.40(10), N1–Cu1–N3 98.93(14), O2–Cu1–N3 95.71(16). Numbers in parentheses are the estimated standard deviation in the least significant digits.

Slow solvent evaporation of a solution of  $[\text{Cu}_2(\text{L}^2\text{O})(\text{BNPP})](\text{CF}_3\text{SO}_3)_2$  (**3**) (Figure 3) gave deep blue crystals suitable for X-ray diffraction analysis. The structure of **3** consists of a binuclear copper(II) complex in which the Cu atoms are bridged together through the BNPP in a bidentate coordination and the alkoxide of the ligand  $\text{L}^2\text{OH}$ . The geometries of the metals are approximately distorted square pyramidal, the  $\tau$  parameter is equal to 0.14 and 0.26 for Cu1 and Cu2, respectively. As in complex **2**, the equatorial positions are occupied by the N atom from a pyridine, the nitrogen and the O atoms of the ethanolamine moiety, as well as the O atom of the BNPP ligand. The apical positions are taken by the nitrogen atoms of the remaining pyridines. The copper to nitrogen distances are slightly longer than in complex **2**: Cu1–N3 2.2432(4) Å and Cu2–N5 2.1864(4) Å. As for **2**, the bases of both pyramids, defined by atoms O1, O3, N1, N2 and O1, O4, N4, N6, respectively, are close to planarity and the out of plane distances of the copper atoms are equal to 0.25 Å and 0.27 Å for Cu1 and Cu2, respectively. The distance between the two copper ions is equal to 3.7252(2) Å which is slightly longer than that observed for complex **2**. This can be explained by the nature of the BNPP ligand which is coordinated to the complex by the two nitrophenyl rings and shows a stabilizing interaction with the  $\text{L}^2\text{OH}$  ligand which is not observed in complex **2**. The phenyl ring of the BNPP ligand, defined by the atoms C38–C43, is involved in a  $\pi$ -stacking interaction with the pyridine, defined by atoms N6, C20–C24. On the an-

other hand, the second nitrophenyl ring of the BNPP ligand is involved in a CH- $\pi$  contact with the two apical pyridines of the  $\text{L}^2\text{OH}$  ligand (the distances between the centroid of the ring, defined by the atoms C32–C37 and the H atoms of C16 and C30, are equal to 3.46 Å and 3.73 Å, respectively). Consequently, the distance between the centroid of the axial pyridines is longer than in complex **2** [ $d = 5.4236(5)$  Å for **3** and  $d = 4.958(4)$  for **2**] and the dihedral angle between both aromatic rings increases from 77° in **2** to 84.18° in **3**.

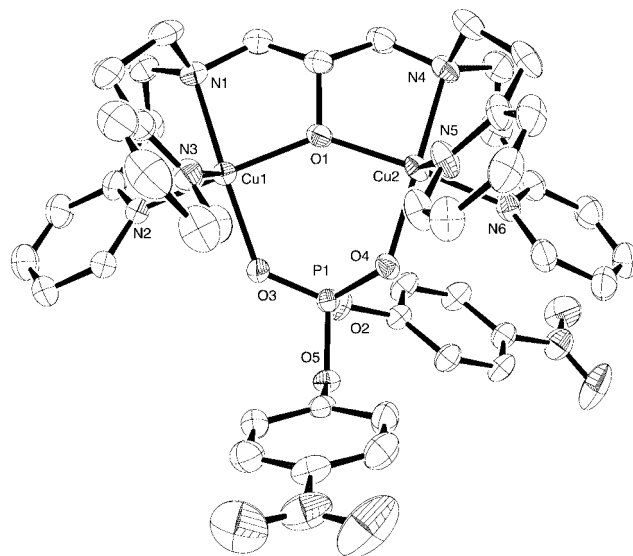


Figure 3. ORTEP perspective view of the copper(II) complex  $[\text{Cu}_2(\text{L}^2\text{O})(\text{BNPP})](\text{CF}_3\text{SO}_3)_2$  (**3**). The H atoms and 2  $\text{CF}_3\text{SO}_3^-$  counterion are omitted for clarity. Bond lengths are in Å: Cu1–O1 1.9823(3), Cu1–O3 1.9854(3), Cu1–N1 2.0628(4), Cu1–N2 2.0116(4), Cu1–N3 2.2432(4), Cu2–O1 1.9874(3), Cu2–O4 1.9733(3), Cu2–N4 2.0595(4), Cu2–N5 2.1864(4), Cu2–N6 2.0230(4). Bond angles are in °: O1–Cu1–O3 92.409(13), O1–Cu1–N1 86.28(2), O1–Cu1–N2 161.41(2), O1–Cu1–N3 102.662(14), O3–Cu1–N1 169.72(2), O3–Cu1–N2 86.358(15), O3–Cu1–N3 94.77(2), N1–Cu1–N2 91.63(2), N1–Cu1–N3 95.47(2), N2–Cu1–N3 95.92(2), O1–Cu2–O4 92.451(12), O1–Cu2–N4 86.62(2), O1–Cu2–N5 106.976(14), O1–Cu2–N6 157.079(15), O4–Cu2–N4 172.71(2), O4–Cu2–N5 91.56(2), O4–Cu2–N6 86.104(15), N4–Cu2–N5 95.63(2), N4–Cu2–N6 91.93(2), N5–Cu2–N6 95.93(2). Numbers in parentheses are the estimated standard deviation in the least significant digits.

**Acid-Base Equilibrium Determination:** The distribution of different species in an aqueous solution is essential for understanding the activity of the complexes in phosphate ester hydrolysis. The protonation constants of the ligands  $\text{L}^1\text{OH}$  and  $\text{L}^2\text{OH}$  (Table 1), as well as the stability constants of their copper complexes and the  $\text{p}K_a$  values of their copper-bound water molecules (Table 2), were determined by potentiometric titration in 0.2 M aqueous KCl at 40 °C.

In the case of  $\text{L}^1\text{OH}$ , three protonation steps were found in the 2–11 pH range. The  $\text{p}K_a$  values of 2.82(2) and 3.89(2) are assigned to the deprotonation of the pyridine N atoms and the third at 7.71(1) to that of the tertiary amine. Deprotonation of the OH group does not occur in the detectable pH range.

Table 1. Protonation constants of the ligands at 40 °C [ $I = 0.2 \text{ M}$  (KCl)].

Species	L <sup>1</sup> OH	pK	L <sup>2</sup> OH
[LH <sub>6</sub> ] <sup>6+</sup>			<<2
[LH <sub>5</sub> ] <sup>5+</sup>			2.66(2)
[LH <sub>4</sub> ] <sup>4+</sup>			3.41(5)
[LH <sub>3</sub> ] <sup>3+</sup>	2.82(2)		4.25(5)
[LH <sub>2</sub> ] <sup>2+</sup>	3.89(2)		5.83(7)
[LH] <sup>+</sup>	7.71(1)		7.92(1)

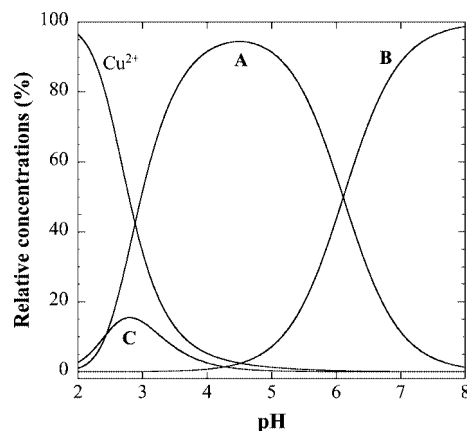
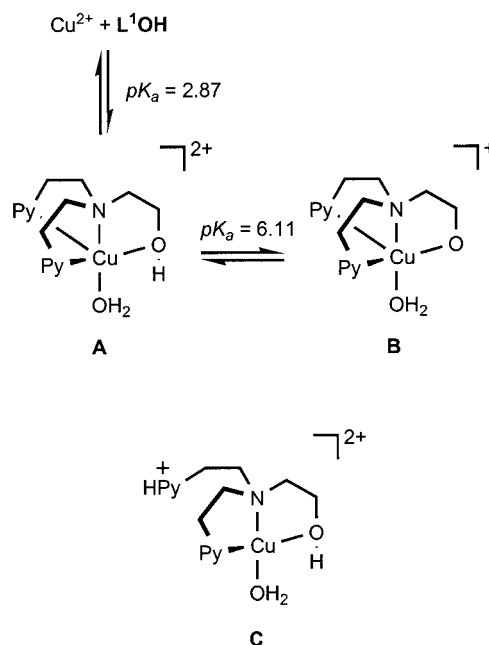
Table 2. Overall stability constants ( $\log\beta$ ) and stepwise deprotonation constants (pK) of the copper complexes at 40 °C [ $I = 0.2 \text{ M}$  (KCl)].

Species	L <sup>1</sup> OH	pK	L <sup>2</sup> OH	pK
	$\log\beta$		$\log\beta$	
{[L <sup>1</sup> OH <sub>2</sub> ]Cu <sub>2</sub> (H <sub>2</sub> O)} <sup>3+</sup> (C)	11.48(8)			
{[L <sup>1</sup> OH]Cu(H <sub>2</sub> O)} <sup>2+</sup> (A)	9.02(3)	2.46		
{[L <sup>1</sup> O]Cu(H <sub>2</sub> O)} <sup>+</sup> (B)	2.91(5)	6.11		
{[L <sup>2</sup> OH]Cu <sub>2</sub> (H <sub>2</sub> O) <sub>2</sub> } <sup>4+</sup> (D)			17.88(2)	
{[L <sup>2</sup> O]Cu <sub>2</sub> (H <sub>2</sub> O) <sub>2</sub> } <sup>3+</sup> (E)			14.14(6)	3.74
{[L <sup>2</sup> O]Cu <sub>2</sub> (H <sub>2</sub> O)(OH)} <sup>2+</sup> (F)			8.0(6)	6.14

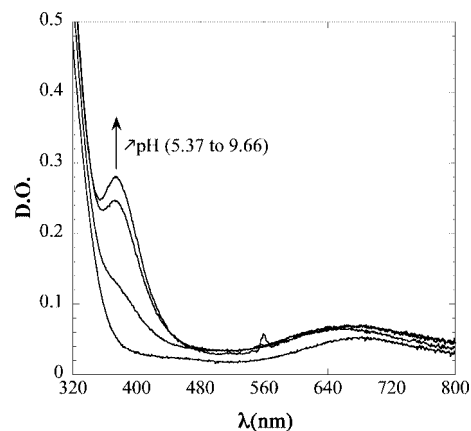
In the case of L<sup>2</sup>OH, three additional deprotonation steps were observed; the first is estimated to occur at a pH less than 2 which is out of the detectable range. In the following steps one proton is removed from each pyridine N atom and the pK<sub>a</sub> values at 5.83(7) and 7.92(1) correspond to the deprotonation of the two tertiary amines. Again, the proton of the OH group is not removed up to pH 11.

Titration of the ligands in the presence of various equivalents of Cu<sup>2+</sup> was also analyzed (Figure 4). In aqueous solution it is reasonable to assume that the bridging triflate anions in **1** and **2** are replaced by water molecules. For the [L<sup>1</sup>OH]:[Cu<sup>2+</sup>] 1:1 system, at a pH higher than 8 and for the [L<sup>1</sup>OH]:[Cu<sup>2+</sup>] 1:2 system at a pH higher than 4, precipitation of copper hydroxide was observed, and neither the mononuclear species at pH > 8 nor the dinuclear species could be determined. Equilibrium modeling from the titration results indicate that two predominant species {[L<sup>1</sup>OH]Cu(H<sub>2</sub>O)}<sup>2+</sup> (A) and {[L<sup>1</sup>O]Cu(H<sub>2</sub>O)}<sup>+</sup> (B) are formed in addition to a small amount of the species (C) (Scheme 2), where one pyridine N atom is protonated. At a pK<sub>a</sub> of 6.11 the ligand OH group in A is deprotonated to give the species {[L<sup>1</sup>O]Cu(H<sub>2</sub>O)}<sup>+</sup> (B). The formation of this species was confirmed by spectrophotometric titration (Figure 5) where an important increase in  $\epsilon$  was observed at 374 nm in the pH range 5.5–7 this was attributed to the formation of the RO–Cu<sup>II</sup> LMCT band ( $\epsilon = 60 \text{ M}^{-1} \text{ cm}^{-1}$  at pH 5.5 and  $\epsilon = 570 \text{ M}^{-1} \text{ cm}^{-1}$  at pH 7). No formation of binuclear species in the pH range examined was observed by ESR spectroscopy.

In the case of L<sup>2</sup>OH, no precipitation of copper hydroxide occurs, and the formation of a dinuclear species starts at a relatively low pH value. The deprotonation of the ligand OH in D is observed at acidic pH (pK = 3.74) which is in agreement with the spectrophotometric titration in this pH range (Figure 6). A distinct peak forms at 365 nm ( $\epsilon =$

Figure 4. Species distribution of the complexes of L<sup>1</sup>OH (5 mM) with 1 equiv. Cu<sup>2+</sup> in 0.2 M KCl at 40 °C.

Scheme 2.

Figure 5. UV/Vis spectra of **1** at various pH values (5.37, 4.83, 7.67 and 9.66).

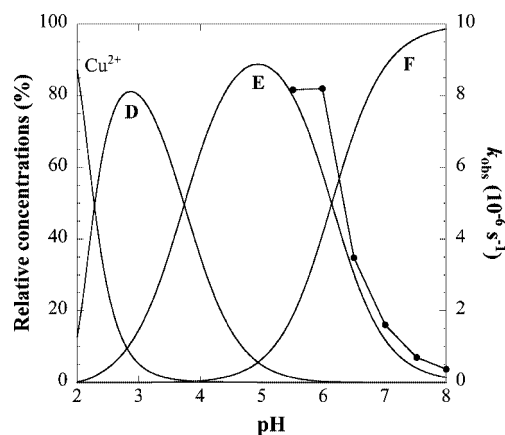


Figure 6. Species distribution of the complexes of  $L^2OH$  (5 mM) with 2 equiv.  $Cu^{2+}$  in 0.2 M KCl at 40 °C and pH/rate profile for BNPP hydrolysis promoted by **2**;  $[2] = 0.488$  mM,  $[BNPP] = 0.192$  mM at 40 °C.

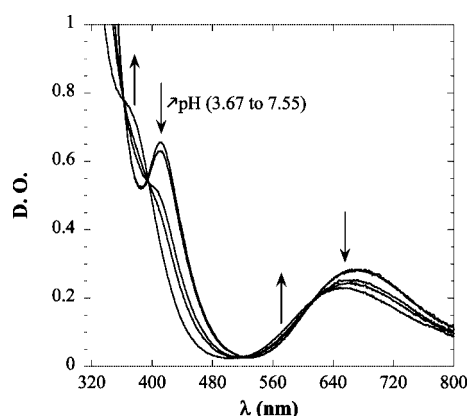


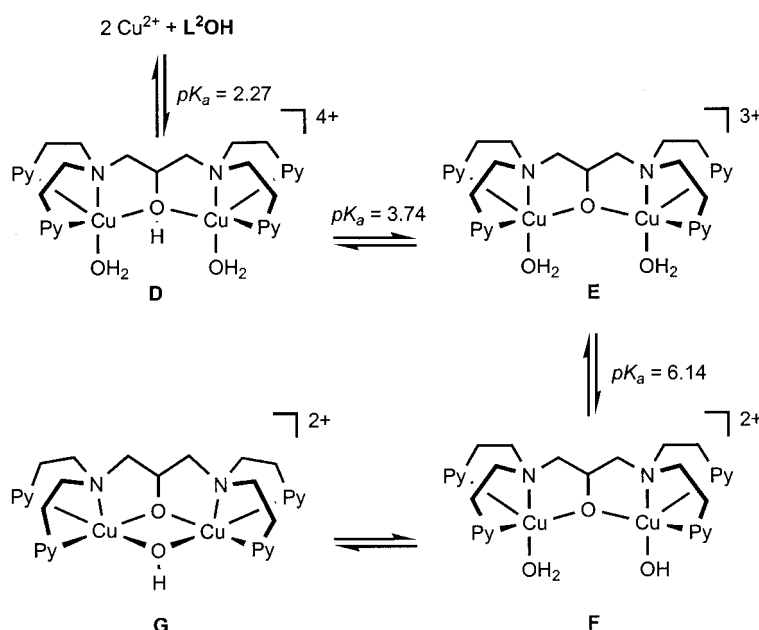
Figure 7. UV/Vis spectra of **2** at various pH values (3.67, 4.53, 5.77, 6.11 and 7.55).

$2100\text{ M}^{-1}\text{ cm}^{-1}$ ) when the pH is raised and it can be assigned as the  $RO-Cu^{II}$  LMCT band. A  $pK_a$  of 6.14 for  $\{[L^2O]-Cu_2OH(H_2O)\}^{2+}$  signifies that the metal-bound water is deprotonated. At this pH, the UV/Visible absorption spectrum shows some variations, the peak at 365 nm becomes a weak shoulder with an important decrease in intensity (Figure 7;  $\epsilon = 1030\text{ M}^{-1}\text{ cm}^{-1}$ ). Similar UV/Visible features have been previously observed for several related ( $\mu$ -pheno)dicopper(II) complexes.<sup>[23,24]</sup> This probably indicates the formation of the double bridged ( $\mu$ -alkoxo)( $\mu$ -hydroxo)-dicopper(II) complex **G**. ESR silent spectra observed at a pH higher than 7, seem to confirm this proposal.

**Phosphate Hydrolysis:** The efficiency of  $[Cu_2(L^2O)](CF_3SO_3)_3$  (**2**) was studied in the 5.5–8 pH range with respect to BNPP hydrolysis and compared to the activity of the parent complex  $[Cu(L^1OH)](CF_3SO_3)_2$  (**1**) (Scheme 3, Table 3). Since, the hydrolysis of BNPP by **1** or **2** proceeds cleanly to give *p*-nitrophenol (PNP) and *p*-nitrophenyl phosphate (MNPP), as revealed by thin-layer chromatography, the progress of the reaction was monitored by the visible absorbance change at 400 nm due to the release of 4-nitrophenolate anion.

Values for the observed initial rate ( $V_i$ ) and the first-order rate ( $k_{obs} = V_i/[BNPP]$ ) constants for the appearance of the *p*-nitrophenolate anion are listed in Table 4 and Table 5 as a function of the pH (Figure 8). While an important effect of pH on the BNPP hydrolysis was observed for **2** (Table 4), the mononuclear complex **1** exhibited only a slight pH effect (Table 5). For **2**, we observed the maximal activity in the 5.5–6 pH range.

In order to find the reactive species, the pH dependence of the initial rate was measured and compared with the species distributions. The plots of  $k_{obs}$  vs. pH give a sigmoidal curve and follow the distribution of the complex  $\{[L^2O]-Cu_2(H_2O)_2\}^{3+}$  (**E**) which must be the active species in the



Scheme 3.

Table 3. Kinetic data for the hydrolysis of BNPP promoted by **2**. Reaction condition: [BNPP] = 0.194 mM, [2] = 0.488 mM, buffer = 50 mM (MES for pH 5.5–6.5, HEPES for pH 7–8), [KCl] = 0.1 M, 40 °C [\*calculated from the hydrolysis of BNPP (1.92 mM) at 40 °C].

pH	$V_i$ $10^{-10} \text{ M s}^{-1}$	$k_{\text{obs}}$ $10^{-6} \text{ s}^{-1}$	$k_2^{[2]}$ $10^{-3} \text{ M}^{-1} \text{ s}^{-1}$	$k_{\text{uncat}}^*$ $10^{-8} \text{ s}^{-1}$	$k_{\text{obs}}/k_{\text{uncat}}$
5.5	15.8	8.10	21	1.36	596
6.0	16.1	8.26	29.4	1.31	630
6.5	6.8	3.49	23.2	1.28	272
7.0	3.14	1.61	26.7	1.24	130
7.5	1.37	0.70	34.5	1.39	50
8.0	0.78	0.40	52.8	2.26	18

Table 4. Kinetic data for the hydrolysis of BNPP promoted by **1**. Reaction condition: [BNPP] = 0.194 mM, [1] = 0.486 mM, buffer = 50 mM (MES for pH 5.5–6.5, HEPES for pH 7–8), [KCl] = 0.1 M, 40 °C.

pH	$V_i$ $10^{-10} \text{ M s}^{-1}$	$k_{\text{obs}}$ $10^{-6} \text{ s}^{-1}$	$k^{[1]}$ $10^{-3} \text{ M}^{-1} \text{ s}^{-1}$	$k_{\text{obs}}^{[2]}/k_{\text{obs}}^{[1]}$
5.5	0.47	0.24	2.62	34
6.0	0.76	0.39	1.79	21
6.5	1.32	0.68	1.97	5
7.0	1.50	0.77	1.80	2
7.5	1.05	0.54	1.16	1.3
8.0	1.0	0.51	1.05	0.8

Table 5. Crystallographic data for the copper(II) complexes **1** and **3**.

Complexes	<b>1</b>	<b>3</b>
<b>Crystal data</b>		
formula	$\text{C}_{18}\text{H}_{21}\text{CuF}_6\text{N}_3\text{O}_7\text{S}_2$	$\text{C}_{45}\text{H}_{45}\text{Cu}_2\text{F}_6\text{N}_8\text{O}_{15}\text{PS}_2$
$M_r$	633.02	1482.106
crystal size	$0.6 \times 0.4 \times 0.2$	$0.5 \times 0.3 \times 0.2$
crystal color	blue	blue
$a$ [Å]	8.4863(4)	10.3462(3)
$b$ [Å]	14.9831(4)	14.0513(6)
$c$ [Å]	10.0586(4)	20.1235(9)
$\alpha$ [°]		94.287(1)
$\beta$ [°]	106.410(1)	102.043(2)
$\gamma$ [°]		107.853(2)
$V$ [Å <sup>3</sup> ]	1226.9(8)	2692.9(2)
$Z$	2	2
$D_{\text{calcd.}}$ [g cm <sup>-3</sup> ]	1.714	1.828
crystal system	monoclinic	triclinic
space group	$P2_1$	$P\bar{1}$
$\mu(\text{Mo-K}\alpha)$ [cm <sup>-1</sup> ]	11.51	13.5
absorption correction	none	none
<b>Data collection</b>		
$T$ [K]	293	293
scan mode	Phi scan	Phi scan
scan width [°]	2	2
$2\theta_{\text{max}}$ [°]	53.74	53.9
unique reflections	2551	9931
<b>Structure refinement</b>		
reflections used for refinement	2551	7827 ( $F_2 > 3\sigma F_2$ )
reflections parameters	333	712
H atoms	calculated	calculated
$R$	0.043	0.043
$R_w$	0.117 <sup>[a]</sup>	0.054 <sup>[b]</sup>
Goodness of fit	1.105	1.76
$\Delta\rho_{\text{fin}}(\text{max./min.})$ [e·Å <sup>-3</sup> ]	0.449/−0.730	0.56/−0.29

[a]  $w = 1/[\sigma^2(F_o^2) + 0.1P^2]$ ,  $P = (F_o^2 + 2F_c^2)/3$ . [b]  $w = 1/[\sigma^2(F_o^2) + 0.03 F_o^2]$ .

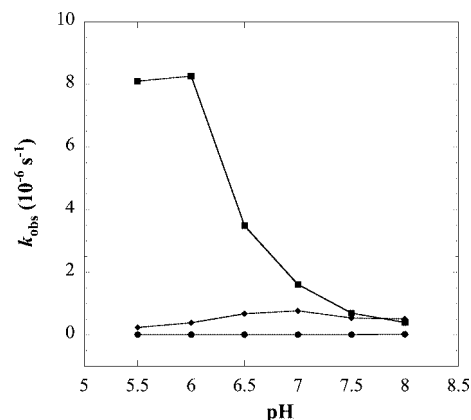


Figure 8. pH dependence on  $k_{\text{obs}}$  for BNPP hydrolysis promoted by copper complexes **1** (filled diamond) and **2** (filled square) and un-promoted (filled circle).

hydrolysis (Figure 5). For this case the second order constants  $k_2$  ( $\text{M}^{-1}\text{s}^{-1}$ ) can be obtained taking into account the quantities of species **E** ( $k_2^{[2]} = k_{\text{obs}}/[\text{E}]$ ) (Table 4).

From these kinetic data, it becomes apparent that: (i) **2** is more efficient in promoting the hydrolysis of BNPP than the mononuclear copper complex **1** (Table 5, ratio  $k_{\text{obs}}^{[2]}/k_{\text{obs}}^{[1]} > 20$ ) and (ii) the rate of the **2**-promoted reaction is up to 600 times faster than the unpromoted reaction. This

means that the copper complex **2** is a good catalyst for phosphate ester hydrolysis in the pH range 5.5–6.0.

In order to gain a better insight into the mechanism, the initial rate was measured as a function of **2** and BNPP concentrations. The rate of BNPP hydrolysis shows a first order dependence on the concentration of the complex **2** (Figure 9). This means that one molecule of **2** is involved in the BNPP hydrolysis. The same result was obtained for complex **1**.

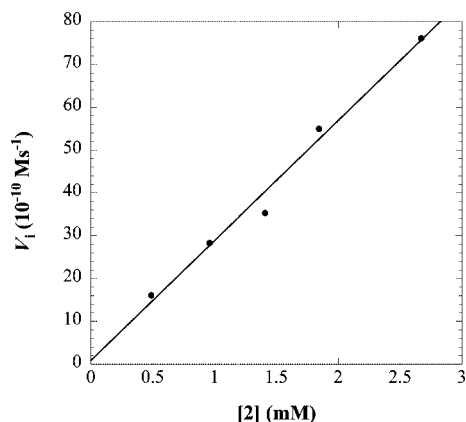


Figure 9.  $V_i$  vs.  $[2]$  of hydrolysis of BNPP. Each reaction mixture contained 50 mM MES/0.1 M KCl, pH 6 at 40 °C and 0.192 mM BNPP. The plotted lines are the computer-generated best fit with  $R = 0.9920$ .

As shown in Figure 10, saturation was observed when the concentration of BNPP was 1 mM. This indicates a pre-equilibrium related to the formation of the active complex (**2**/substrate) followed by the rate-determining transformation of the substrate with the complex. The treatment of the data, using the Michaelis–Menten model, showed the following constants:  $K_M = 0.17$  mM and  $k_{cat} = 11.2 \cdot 10^{-6} \text{ s}^{-1}$ . For the complex **1** (0.5 mM) at pH 7,  $K_M = 0.65$  mM

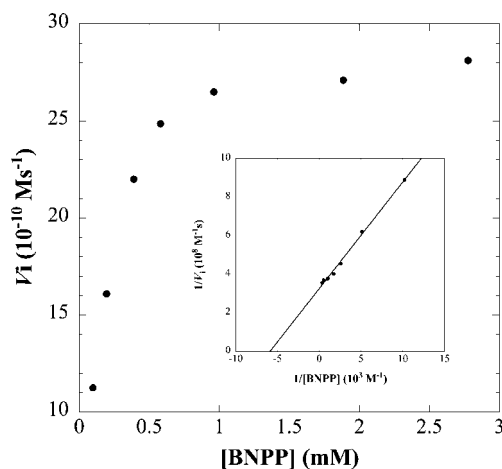


Figure 10. Saturation kinetics of copper complex **2** by BNPP. Each reaction mixture contained 50 mM MES/0.1 M KCl, pH 6 at 40 °C and 0.5 mM **2**. Inset: Lineweaver–Burk plot, the plotted line is the computer-generated best fit ( $R = 0.9978$ ) according to  $1/V_i = K_M/(V_{max}[\text{BNPP}]) + 1/V_{max}$ , where  $K_M = 0.17$  mM,  $V_{max} = 3.07 \cdot 10^{-9} \text{ M s}^{-1}$  and  $k_{cat} = 11.2 \cdot 10^{-6} \text{ s}^{-1}$ ,  $\{[\text{L}^2\text{O}]\text{Cu}_2(\text{H}_2\text{O})_2\}^{3+} = 0.55[2]$ .

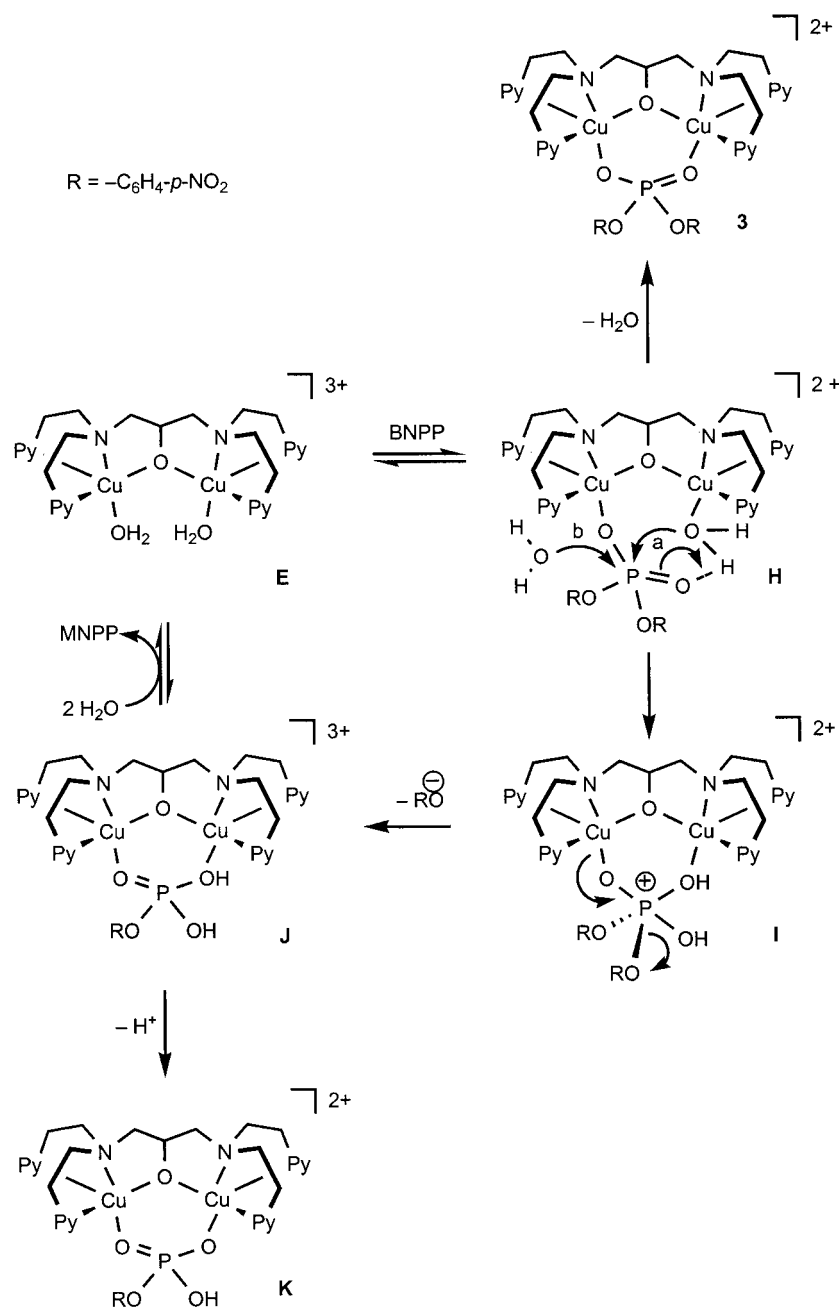
and  $k_{cat} = 1.38 \cdot 10^{-6} \text{ s}^{-1}$  were obtained taking  $\{[\text{L}^1\text{O}]\text{Cu}(\text{H}_2\text{O})\}^+$  = 0.89[1].

On the basis of the potentiometric titration study and kinetic data we assume that the bis(aqua)copper complex  $\{[\text{L}^2\text{O}]\text{Cu}_2(\text{H}_2\text{O})_2\}^{3+}$  (**E**) is responsible for the BNPP hydrolysis (Figure 5) according to a double Lewis acid activation mechanism. As shown in Scheme 4, the cleavage process may involve the following steps: (i) the phosphodiester BNPP coordinates to one copper ion as a monodentate ligand by replacing one water molecule (**E** → **H**); (ii) deprotonation of the second water ligand by a phosphate group and the subsequent nucleophilic attack of the phosphate by hydroxide leads to a pentavalent intermediate (**H** → **I**). Nucleophilic attack by free water molecule (Scheme 4, pathway b) can be excluded since the dinuclear complex **2** is more efficient in promoting hydrolysis of BNPP than the mononuclear complex **1** (Table 4, ratio  $k_{obs}^{[2]}/k_{obs}^{[1]} > 20$ ); (iii) the P–O bond breaks to give *p*-nitrophenolate followed by the formation of the monoester complex (**I** → **J**); (iv) replacement of MNPP by water leads to the active species (**J** → **E**). This mechanism is in good agreement with the results described in the literature. It is generally believed that one of the metal ions serves to reversibly bind the phosphoester substrate whereas the second ion serves to activate a hydroxide ion at a physiological pH. The second metal ion also serves to increase the electrophilic susceptibility of the substrate and neutralizes the anionic substrate, thus moderating the electrostatic repulsion of the attacking nucleophile. The reaction then consists of an intramolecular nucleophilic attack of the adjacent hydroxide at the substrate (P–O bond cleavage).

Other pathways that should be considered are the formation of a bridged phosphate complex **3** (**K**). Due to an appropriate Cu–Cu distance, the formation of these complexes is favorable and stabilizes the phosphate ester. Indeed, complex **3** was prepared independently and under the reaction conditions (40 °C, 50 mM MES pH 6) it was not hydrolysed into *p*-nitrophenol and *p*-nitrophenyl phosphate even after 3 h. The easy formation and stability of such intermediates limits the performance of the catalyst. The copper(II) complex **2** behaves like ribonuclease which, in addition to a correct enzyme–substrate complex, also forms non-reactive enzyme–substrate complexes that do not form products but inhibit the reactions.

## Conclusion

We have demonstrated that the dinuclear complex **2** hydrolyzes the activated phosphodiester BNPP 20-fold faster than the mononuclear complex **1** and up to 600-fold faster than the un-promoted reaction at a slightly acidic pH (pH 6). The mechanism for the hydrolysis of BNPP appears to be classic according to a double Lewis acid activation. Our results are interesting for the design of more efficient copper catalysts for hydrolysis of phosphodiester. What should be solved next is (i) the stabilization of the species **F** in preventing the formation of a double bridged ( $\mu$ -alk-



Scheme 4. Proposed mechanism for BNPP hydrolysis promoted by the copper complex **2**.

oxo)( $\mu$ -hydroxo)dicopper(II) complex **G** which seems not reactive in the hydrolysis of BNPP; (ii) to solve the problem of product (substrate) inhibition in preventing the formation of species such as **K** (**3**). Ligands, which could solve these problems, are currently under investigation in our laboratory.

## Experimental Section

**General Remarks:** NMR spectra were recorded at 25 °C in CDCl<sub>3</sub> using a Bruker AC-300 spectrometer. Chemical shifts are reported in ppm as  $\delta$  values downfield from an internal standard of TMS. Infrared spectra were measured using neat films or KBr pellets

using a Specord M80 (Carl Zeiss Jena) instrument. UV/Vis absorption spectra were recorded in CH<sub>2</sub>Cl<sub>2</sub> using a Shimadzu UV-120A spectrometer. Elemental analyses were measured using a C, H, N, S Carlo Erba EA 1108 analyzer.

**Materials:** Solvents were freshly distilled under Ar (MeOH/Mg, Et<sub>2</sub>O/Na-benzophenone ketyl, acetone/CaH<sub>2</sub> and CH<sub>2</sub>Cl<sub>2</sub>/P<sub>2</sub>O<sub>5</sub>). Commercial starting materials were used without purification, except for 2-vinylpyridine which was chromatographed using silica gel prior to use. Ligand **L**<sup>2</sup>OH was prepared by the Michael addition of 1,3-diamino-2-hydroxypropane to 2-vinylpyridine.<sup>[17]</sup> Complex [Cu<sub>2</sub>(**L**<sup>2</sup>O)](CF<sub>3</sub>SO<sub>3</sub>)<sub>3</sub> (**2**) was prepared by the reaction of Cu(CF<sub>3</sub>SO<sub>3</sub>)<sub>2</sub> with the ligand **L**<sup>2</sup>OH in CH<sub>2</sub>Cl<sub>2</sub>.<sup>18</sup>

**N,N-Bis[2-(2-pyridyl)ethyl]ethanolamine (**L**<sup>1</sup>OH):** 2-Ethanolamine (1.83 g, 1.81 mL, 30 mmol) and 2-vinylpyridine (25.2 g, 25.9 mL,

0.24 mol) were heated under reflux in MeOH (150 mL) with acetic acid (4.41 g, 4.2 mL, 73.5 mmol) for 5 days. Methanol was evaporated under vacuum. The resulting brown mixture was dissolved in CH<sub>2</sub>Cl<sub>2</sub> (100 mL), washed with 15% aqueous NaOH (2 × 50 mL) and brine (2 × 50 mL). The organic layer was dried with Na<sub>2</sub>SO<sub>4</sub>. The solvent was removed by rotary evaporation to give an oil. This oil was dried under vacuum (ca. 0.01 Torr) at 40 °C to remove excess 2-vinylpyridine. The residue was chromatographed on silica gel (CH<sub>2</sub>Cl<sub>2</sub>/MeOH, 85:15) to yield the pure ligand **L<sup>1</sup>OH**. Yield: 6.18 g, 76%. <sup>1</sup>H NMR (200 MHz, CDCl<sub>3</sub>): δ = 2.60 (t, *J* = 5.1 Hz, 2 H), 2.70–2.90 (m, 8 H), 3.40 (t, *J* = 5.1 Hz, 2 H), 6.85–7.0 (m, 4 H), 7.40 (td, *J* = 5.8 Hz and *J* = 1.7 Hz, 2 H), 8.40 (dd, *J* = 3.1 Hz and *J* = 1.0 Hz, 2 H) ppm. <sup>13</sup>C NMR (50 MHz, CDCl<sub>3</sub>): δ = 35.8 (CH<sub>2</sub>), 53.9 (CH<sub>2</sub>), 55.9 (CH<sub>2</sub>), 59.4 (CH<sub>2</sub>), 121.0 (CH<sub>py</sub>), 123.3 (CH<sub>py</sub>), 136.2 (CH<sub>py</sub>), 148.9 (CH<sub>py</sub>), 160.3 (C<sub>py</sub>) ppm. IR (neat film):  $\tilde{\nu}$  = 3300 (ν<sub>OH</sub>), 3010 (ν<sub>C-H</sub> aromatic), 2900 (ν<sub>C-H</sub> aliphatic), 1600, 1570, 1480, 1440 (ν<sub>C-C</sub> pyridine ring), 1055 (ν<sub>C-O</sub>), 770, 756 (γ<sub>C-H</sub>, γ<sub>C-C</sub> aromatic) cm<sup>-1</sup>. UV/Vis (MeOH): λ<sub>max</sub>/nm (ε/M<sup>-1</sup> cm<sup>-1</sup>) = 230 (4200), 260 (7700).

**[Cu(L<sup>1</sup>OH)](CF<sub>3</sub>SO<sub>3</sub>)<sub>2</sub> (1):** Ligand **L<sup>1</sup>OH** (590 mg, 2 mmol) dissolved in CH<sub>2</sub>Cl<sub>2</sub> (10 mL) was added dropwise to a suspension of Cu(CF<sub>3</sub>SO<sub>3</sub>)<sub>2</sub> (723.4 mg, 2 mmol) in CH<sub>2</sub>Cl<sub>2</sub> (10 mL). After stirring at room temperature for 2 h, a deep blue oil was formed. This oil was allowed to settle and washed with Et<sub>2</sub>O until the formation of a solid. Drying under vacuum afforded the copper(II) complex **1**. Yield: 786 mg, 63%. IR (KBr):  $\tilde{\nu}$  = 3450 (ν<sub>O-H</sub>), 3020 (ν<sub>C-H</sub> aromatic), 2920 (ν<sub>as C-H</sub> aliphatic), 1615, 1500, 1450, (ν<sub>C-C</sub> pyridine), 770, 740 (γ<sub>C-H</sub> aromatic, γ<sub>C-C</sub>), 1270, 1035, 640, 518 (ν<sub>triflate</sub>) cm<sup>-1</sup>. UV/Vis (MeOH): λ<sub>max</sub>/nm (ε/M<sup>-1</sup> cm<sup>-1</sup>) = 215 (4130), 262 (9650), 381 (220), 690 (120). C<sub>18</sub>H<sub>21</sub>N<sub>3</sub>CuF<sub>6</sub>O<sub>7</sub>S<sub>2</sub> (633.02): calcd. C 34.20, N 6.65, H 3.32, Cu 10.95; found C 34.85, N 6.42, H 3.24, Cu 10.25.

**[Cu<sub>2</sub>(L<sup>2</sup>O)(BNPP)](CF<sub>3</sub>SO<sub>3</sub>)<sub>2</sub> (3):** To a solution of the complex **2** (54.2 mg, 0.05 mmol) in H<sub>2</sub>O (10 mL) was added BNPP (17 mg, 0.05 mmol) dissolved in MeOH (5 mL). After stirring at room temperature for 2 h, the solvent was allowed to evaporate in air. Deep blue crystals suitable for X-ray diffraction were grown within a few days. Yield: 44 mg, 69%. IR (KBr):  $\tilde{\nu}$  = 3120, 3080 (ν<sub>C-H</sub> aromatic), 2920 (ν<sub>as C-H</sub> aliphatic), 2880 (ν<sub>s C-H</sub> aliphatic), 1610, 1590, 1490 (ν<sub>C-C</sub> pyridine), 1520 (ν<sub>as NO<sub>2</sub></sub>), 1355 (ν<sub>s NO<sub>2</sub></sub>), 1220 (ν<sub>as P-O-C</sub> aromatic), 1150 (ν<sub>C-O</sub>), 770–750 (γ<sub>C-H</sub>, γ<sub>C-C</sub> aromatic), 1265, 1034, 640, 518 (ν<sub>triflate</sub>) cm<sup>-1</sup>. C<sub>45</sub>H<sub>45</sub>N<sub>8</sub>Cu<sub>2</sub>O<sub>15</sub>F<sub>6</sub>S<sub>2</sub>P (1273.08): calcd. C 42.40, N 8.80, H 3.53, Cu 9.98; found C 41.95, N 8.58, H 3.27, Cu 10.42.

**pH Potentiometric Titration:** The pH potentiometric titrations were conducted at 40.0 ± 0.1 °C at an ionic strength of 0.2 M KCl. Calibration of the electrode and pH meter was performed using a 0.05 M KH/phthalate buffer and a pK<sub>w</sub> of 13.294 at 40 °C. Solution of ligands **L<sup>1</sup>OH** and **L<sup>2</sup>OH** (5 mM) in 0.2 M KCl, acidified with HCl (0.2008 M), were titrated in an N<sub>2</sub> atmosphere with KOH solution (0.1941 M) at 40 °C in the presence and absence of Cu<sub>2</sub>(CF<sub>3</sub>SO<sub>3</sub>)<sub>2</sub>. The initial concentration of Cu<sub>2</sub>(CF<sub>3</sub>SO<sub>3</sub>)<sub>2</sub> was varied between 4–10 mM. The titrations of the free ligands were run between pH 2 and 11.5, with added metal solution between pH 2 and 8 for the ligand **L<sup>1</sup>OH** and between pH 2 and 11 for the ligand **L<sup>2</sup>OH**. To calculate the deprotonation constants and Cu<sup>II</sup> association constants from the titration data a multiparameter curve fitting program based on SUPERQUAD<sup>[25]</sup> and PSEQUAD<sup>[26]</sup> was used.

**Kinetics:** Hydrolysis of BNPP was monitored by following the visible absorption change at 400 nm (ε = 18500 M<sup>-1</sup> cm<sup>-1</sup>) due to the release of *p*-nitrophenolate anion (PNPate). Conversion from absorbance to concentration was performed by using the Lambert–

Beer law [Equation (1)]. In order to take into account the concentration change of the PNPate as a function of pH, the [PNPate]<sub>tot</sub> was calculated following equations (2) and (3), where the pK<sub>a</sub> of PNP (7.15) was determined using the above condition. The activity of the complex was determined by the initial rate method.

$$[\text{PNPate}]_{\text{meas}} = O. D./18500 \quad (1)$$

$$\text{pH} = 7.15 + \log([\text{PNPate}]_{\text{meas}}/[\text{PNP}]) \quad (2)$$

$$[\text{PNPate}]_{\text{tot}} = [\text{PNPate}]_{\text{meas}} + [\text{PNP}] \quad (3)$$

In a typical kinetic experiment, freshly prepared phosphate ester stock solution in water (12 μL, 50 mM) was added to a solution of copper(II) complex (**1**: 75 μL, 20 mM; **2** 60 μL, 25 mM) at 40 °C. The copper complex solutions were buffered with MES (pH 5.5–6.5), HEPES (pH 7–8) and the ionic strength was maintained with 0.1 M KCl. The final volume was 3 mL. The pseudo-first-order rate constants for un-promoted reactions (*k*<sub>uncat</sub>, s<sup>-1</sup>) were measured by following the increase in absorbance from a 1.92 mM BNPP solution.

**X-ray Crystallographic Studies:** All the measurements were performed using a Bruker–Nonius KappaCCD diffractometer.<sup>[27]</sup> The cell determinations and data integrations were performed using the software Denzo-Scalepak.<sup>[28]</sup> The structure solutions were obtained using Sir92<sup>[29]</sup> and the refinements were carried out using SHELXL-97,<sup>[30]</sup> except for complex **3**, which was refined using the software MaxXus (Table 5).<sup>[31]</sup>

CCDC-283857 (for **1**), -283855 (for **2**) and -283856 (for **1**) contain the supplementary crystallographic data for this paper. These data can be obtained free of charge from The Cambridge Crystallographic Data Centre via www.ccdc.cam.ac.uk/data\_request/cif.

## Acknowledgments

This research was supported by the CNRS, the Ministère de la Recherche et de la Technologie (Balaton program), the Hungarian Research Fund (OTKA # 43414), and the Ministère des Affaires Étrangères (grant for K. S.). The authors are grateful to Dr. A. Heumann for a number of enlightening discussions.

- [1] E. L. Hegg, J. N. Burstyn, *Coord. Chem. Rev.* **1998**, *173*, 133–165.
- [2] A. Sreedhara, J. A. Cowan, *J. Biol. Inorg. Chem.* **2001**, *6*, 337–347.
- [3] D. E. Wilcox, *Chem. Rev.* **1996**, *96*, 2435–2458.
- [4] E. E. Kim, H. W. Wyckoff, *J. Mol. Biol.* **1991**, *218*, 449–464.
- [5] T. Klabunde, N. Strater, R. Frohlich, H. Witzel, B. Krebs, *J. Mol. Biol.* **1996**, *259*, 737–748.
- [6] R. Hettich, H.-J. Schneider, *J. Am. Chem. Soc.* **1997**, *119*, 5638–5647.
- [7] N. H. Williams, W. Cheung, J. Chin, *J. Am. Chem. Soc.* **1998**, *120*, 8079–8087.
- [8] B. K. Takasaki, J. Chin, *J. Am. Chem. Soc.* **1994**, *116*, 1121–1122.
- [9] M. E. Branum, A. K. Tipton, S. Zhu, L. Que Jr, *J. Am. Chem. Soc.* **2001**, *123*, 1898–1904.
- [10] T. Koike, E. Kimura, in: *Advances in Inorganic Chemistry* (Ed.: A. G. Sykes), Academic Press, San Diego, CA, **1996**, vol. 44, pp. 229–261.
- [11] T. Koike, M. Inoue, E. Kimura, M. Shiro, *J. Am. Chem. Soc.* **1996**, *118*, 3091–3099.

- [12] F. Verge, C. Lebrun, M. Fontecave, S. Ménage, *Inorg. Chem.* **2003**, *42*, 499–507.
- [13] A. Sreedhara, J. D. Freed, J. A. Cowan, *J. Am. Chem. Soc.* **2000**, *122*, 8814–8824.
- [14] T. Gajda, Y. Düpre, I. Török, J. Harmer, A. Schweiger, J. Sander, D. Kuppert, K. Hegetschweiler, *Inorg. Chem.* **2001**, *40*, 4918–4927.
- [15] K. M. Deck, T. A. Tseng, J. N. Burstyn, *Inorg. Chem.* **2002**, *41*, 669–677.
- [16] F. H. Fry, A. J. Fischmann, M. J. Belousoff, L. Spiccia, J. Brügger, *Inorg. Chem.* **2005**, *44*, 941–950.
- [17] K. D. Karlin, Z. Tyeklár, A. Farooq, M. S. Haka, P. Ghosh, R. W. Cruse, Y. Gultneh, J. C. Hayes, P. J. Toscano, J. Zubieta, *Inorg. Chem.* **1992**, *31*, 1436–1451.
- [18] K. Selmececi, M. Réglér, M. Giorgi, G. Speier, *Coord. Chem. Rev.* **2003**, *245*, 191–201.
- [19] A. W. Addison, H. M. J. Hendriks, J. Reedijk, L. K. Thomson, *Inorg. Chem.* **1981**, *20*, 103–110.
- [20] K. D. Karlin, I. Sanyal, A. Farooq, R. R. Jacobson, S. N. Shaikh, J. Zubieta, *Inorg. Chim. Acta* **1990**, *174*, 13–15.
- [21] K. D. Karlin, J. Shi, J. C. Hayes, J. W. McKown, J. P. Hutchinson, J. Zubieta, *Inorg. Chim. Acta* **1984**, *91*, L3–L7.
- [22] K. D. Karlin, A. D. Zuberbühler, in: *Bioinorganic Catalysis* (Eds.: J. Reedijk, E. Bouwman), 2<sup>nd</sup> ed., Marcel Dekker, New York, **1999**, pp. 469–534.
- [23] J. J. Maloney, M. Glogowski, D. F. Rohrbach, F. L. Urbach, *Inorg. Chim. Acta* **1987**, *127*, L33–L35.
- [24] S. Torelli, C. Belle, I. Gautier-Luneau, J. L. Pierre, E. Saint-Aman, J.-M. Latour, L. Le Pape, D. Luneau, *Inorg. Chem.* **2000**, *39*, 3526–3536.
- [25] L. Zékány, I. Nagypál, in: *Computational Methods for the Determination of Stability Constants* (Ed.: D. L. Leggett), Plenum Press, New York, **1985**, pp. 291–353.
- [26] P. Gans, A. Sabatini, A. Vacca, *J. Chem. Soc., Dalton Trans.* **1985**, 1195–1200.
- [27] Bruker-Nonius, Kappa CCD Reference Manual, Nonius B. V., P. O. Box 811, 2600 Av, Delft, The Netherlands, **1998**.
- [28] Z. Otwinowski, W. Minor, in: *Methods in Enzymology* (Eds.: C. W. Carter Jr, R. M. Sweet), Academic Press, vol. 276, pp. 307–326, **1997**.
- [29] A. Altomare, G. Cascarano, C. Giacovazzo, A. Guagliardi, M. C. Burla, G. Polidori, M. Camalli, *J. Appl. Crystallogr.* **1994**, *27*, 435.
- [30] G. M. Sheldrick, *SHELXL-97*, University of Göttingen, **1997**.
- [31] S. Mackay, C. J. Gilmore, C. Edwards, M. Tremayne, N. Stewart, K. Shankland, *MaXus: a computer program for the solution and refinement of crystal structures from diffraction data*; University of Glasgow, Scotland, UK, Nonius BV, Delft, The Netherlands and MacScience Co. Ltd., Yokohama, Japan, **1998**.

Received: July 5, 2005

Published Online: January 9, 2006